

Quantitative Image-Based Physical Analysis of Lung Microstructure from HRCT for Automated Disease Stratification

Mehrun Nisa¹, Muhammad Saeed Ahmad², Aliza Nadeem¹, Ayesha Amjad¹, Sehar Zafar¹, Aneeba Kanwal¹, Warda Afifa¹, Nimra Ejaz¹, Hafiz Muhammad Amir Jamil³, Naima Amin⁴

¹Department of Physics, Government Sadiq College Women University, Bahawalpur, Pakistan

²Department of Computer Science & IT, Government Sadiq College Women University, Bahawalpur, Pakistan

³Senior Registrar, Bahawal Victoria Hospital, Bahawalpur, Pakistan

⁴Department of Physics, COMSATS University Islamabad, Lahore Campus, Pakistan

Corresponding Author: Naima Amin Email: naimaamin@ciitlahore.edu.pk

ABSTRACT

In this study, quantitative texture analysis of HRCT lung images was performed using MaZda software to classify and compare Tubular Bronchiectasis, COPD, Hydropneumothorax, Pleural Effusion, Hypersensitivity Pneumonitis, and Interstitial Lung Disease (ILD) with normal lung tissue. A total of 127 samples obtained from 41 patients were analyzed to ensure broad representation across diagnostic categories. More than 300 texture features were extracted from selected Regions of Interest (ROIs), and the POE+ACC method was used to identify the ten most discriminative features. These selected features were evaluated using Principal Component Analysis (PCA), Linear Discriminant Analysis (LDA), and Nonlinear Discriminant Analysis (NDA). All three methods achieved 0% misclassification error, demonstrating excellent feature stability and reproducibility. LDA showed strong linear clustering, NDA produced superior nonlinear discrimination using a one-class Artificial Neural Network (ANN), and PCA effectively visualized class variance and consistent grouping. The results confirm that MaZda-based texture analysis offers an accurate, objective, and non-invasive tool capable of distinguishing a wide range of pulmonary diseases using HRCT, supporting radiological decision-making and improving diagnostic precision.

KEYWORDS

HRCT Radiomics, Texture Analysis, Pulmonary Disease Classification, MaZda Software, Machine Learning

1. Introduction

The lungs primarily function as the organ of gas exchange between alveoli and blood and also contribute to immune defense and metabolic homeostasis through particle clearance and enzymatic neutralization of biological agents [1]. Chronic lung diseases remain major causes of global morbidity and mortality, arising from multifactorial contributors such as smoking, environmental pollution, and occupational exposures [2]. Chronic Obstructive Pulmonary Disease (COPD) is a progressive disorder characterized by airflow limitation and structural remodeling of the airways, with emphysema and chronic bronchitis representing its dominant phenotypes [3]. Tubular bronchiectasis involves irreversible dilatation of bronchi due to

chronic infection or inflammation, leading to mucus retention, recurrent infections, and persistent cough [4]. Interstitial lung diseases (ILDs) represent a broad category of diffuse parenchymal abnormalities that may progress to fibrosis, impaired diffusion capacity, and respiratory failure [5]. Hypersensitivity pneumonitis (HP) results from repeated inhalation of immunogenic particles and is characterized by interstitial inflammation, ground-glass opacities, and fibrosis in chronic stages [6]. Pleural effusion involves the accumulation of excess fluid in the pleural cavity and often causes dyspnea and chest discomfort, whereas hydropneumothorax comprises simultaneous air and fluid in the pleural space, posing risks of respiratory compromise [7].

High-Resolution Computed Tomography (HRCT) is the primary imaging modality for detailed evaluation of lung and pleural abnormalities because it acquires thin-section (~1.0–1.5 mm) images with higher spatial resolution than conventional CT, enabling early visualization of airway changes, interstitial thickening, parenchymal destruction, nodules, pleural collections, and fibrotic patterns that are often not detectable on standard imaging [8]. Over the last decade, HRCT radiomics has emerged as a powerful technique for quantifying subtle texture patterns that may reflect microstructural changes in lung tissue, offering reliable biomarkers for diagnosis, prognosis, and disease phenotyping [9].

In computer vision, texture analysis is fundamental for medical image interpretation, pattern recognition, defect detection, and quantitative morphological assessment. Statistical texture analysis methods evaluate the distribution of pixel intensities to characterize underlying tissue structure objectively [10]. Based on the number of pixels used in computation, texture methods are classified into first-order (single-pixel statistics), second-order (relationships between pixel pairs), and higher-order (patterns among three or more pixels). First-order statistics quantify global intensity properties such as mean and variance, whereas second- and higher-order statistics capture spatial interactions between neighboring pixels, enabling richer description of tissue heterogeneity.

Machine learning has become integral to medical image analysis because it enables automated pattern recognition and enhances diagnostic precision through data-driven learning [11]. Radiomics-based classifiers such as neural networks, linear discriminant analysis, and nonlinear discriminant algorithms have been increasingly used to detect subtle disease-specific texture patterns on HRCT. MaZda software is a widely used platform for quantitative biomedical texture analysis, offering extraction of hundreds of features from multiple statistical families, including histogram, GLCM, run-length, gradient, and autoregressive features. Its feature selection tools, such as Probability of Classification Error + Average Correlation Coefficient (POE+ACC), reduce redundancy and identify the most discriminative radiomic descriptors for disease classification.

Despite increasing use of HRCT radiomics in pulmonary imaging, most prior studies have focused on single disease entities or limited disease groups and have rarely applied a unified texture-analysis and feature-selection framework across multiple pulmonary and pleural disorders. In particular, there is a lack of comparative evaluation of linear and nonlinear discriminant classifiers using robust MaZda-based radiomic features. This methodological gap limits the generalizability and clinical translation of existing radiomics models. The present study addresses this gap by applying a standardized MaZda-based texture-analysis pipeline with POE+ACC feature selection and comparative PCA, LDA, and ANN-based NDA classification across a broad spectrum of lung and pleural diseases.

2. Materials and Methods

A total of 127 samples were obtained from 41 patients with clinically and radiologically diagnosed lung diseases for texture analysis. The patients (aged 20–80 years, male and female) were diagnosed with COPD

(including emphysema and chronic bronchitis), tubular bronchiectasis, pleural effusion, hydropneumothorax, hypersensitivity pneumonitis, and interstitial lung disease. HRCT scans were acquired using an AQ-Prime CT scanner (Serial No. BCA1492054) at the Radiology Department of Sadiq Abbasi Hospital, Bahawalpur. Patients younger than 20 years and those with lung malignancies, metastatic disease, active tuberculosis, granulomatous infections, or a history of thoracic surgery were excluded. All DICOM images were converted into Bitmap format using MicroDicom software for texture extraction in MaZda.

2.1. Region of Interest (ROI) and Feature Extraction

The first step involved importing, formatting, and preparing digital HRCT images for texture analysis. Regions of Interest (ROIs) were manually selected from diagnostically relevant locations to ensure meaningful feature extraction and reduce unnecessary computational load [10].

Both first-order and second-order statistics were evaluated. First-order statistics (histogram features) quantify pixel-intensity distribution without considering spatial relationships. Second-order statistics, derived from the Gray Level Co-occurrence Matrix (GLCM), quantify spatial dependencies and remain widely used for lung texture characterization due to their ability to capture heterogeneity and structural distortion [11].

Additional features included Run-Length Matrix (RLM/GLRLM) for coarseness and fineness, gradient-based features for edge behaviour, and autoregressive (AR) features that model pixel intensities as functions of neighbouring patterns. To reduce acquisition-related variability, $\pm 3\sigma$ intensity normalization was applied to each ROI, a method proven effective in stabilizing radiomic features across heterogeneous data sets [12].

2.2. Feature Selection and Dimensionality Reduction

Feature selection was performed using the Probability of Classification Error + Average Correlation Coefficient (POE+ACC) method, which identifies features with the lowest classification error and minimal redundancy. Recent radiomics studies have shown that POE+ACC improve classification accuracy by retaining only the most discriminative features for lung disease analysis [13].

2.3. Feature Classifiers

Selected features were analysed using Principal Component Analysis (PCA), Linear Discriminant Analysis (LDA), and Nonlinear Discriminant Analysis (NDA). LDA enhances linear class separation and has demonstrated high accuracy in HRCT texture-based lung disease classification. NDA, implemented with a one-class Artificial Neural Network (ANN), captures nonlinear boundaries and has been shown to improve classification in complex radiomics datasets [14]. Whereas PCA provides unsupervised dimensionality reduction by projecting features onto components representing the largest variance in the data.

2.4. Feature Analysis

PCA, LDA, and NDA were applied to the ten POE+ACC-selected features to evaluate their discriminative ability. PCA assisted in variance visualization, LDA provided linear separation between disease classes, and NDA further captured nonlinear separability.

2.5. Analytical Framework

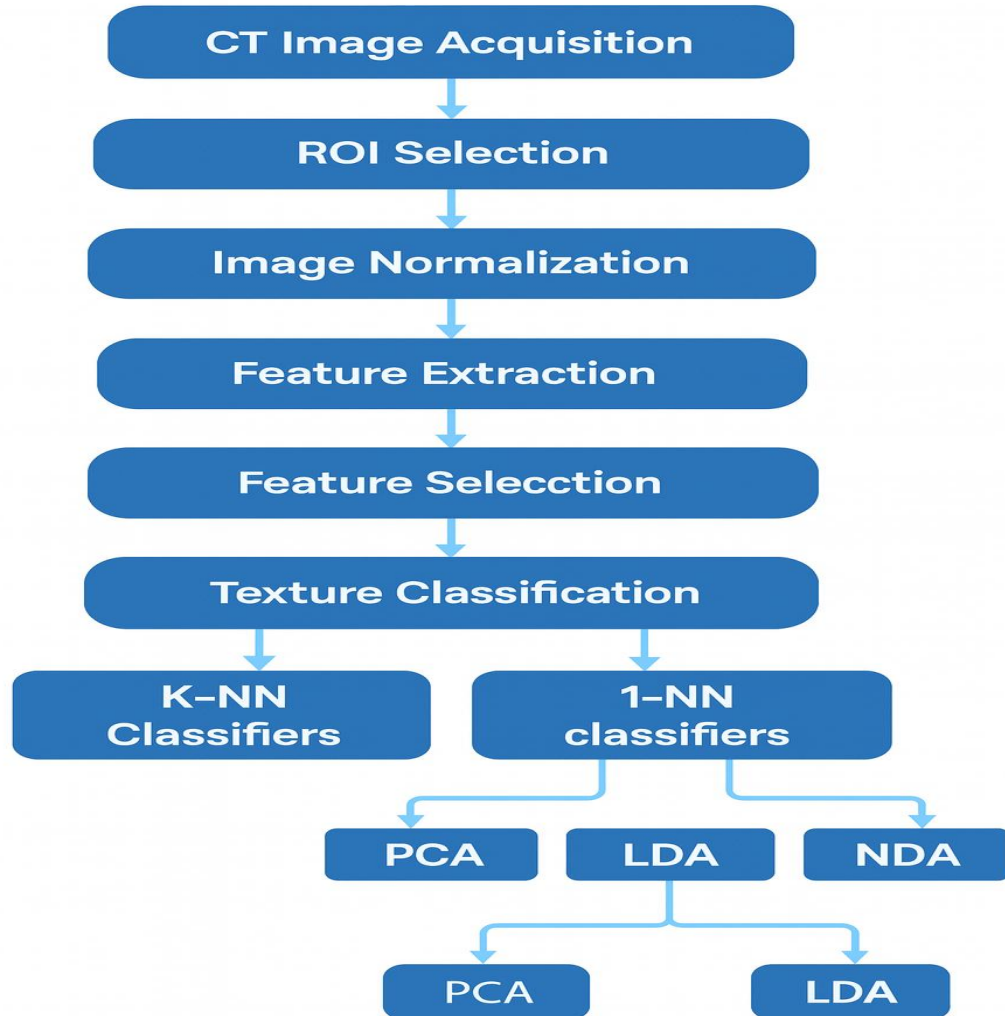


Figure 1 Workflow of Texture Analysis from Image Acquisition to Classification

The POE+ACC feature selection method was adopted to determine the ten most discriminative features. The ACC component removed highly correlated features, while the POE component minimized misclassification probability. Together, these ensured strong class discrimination and reliable outcomes.

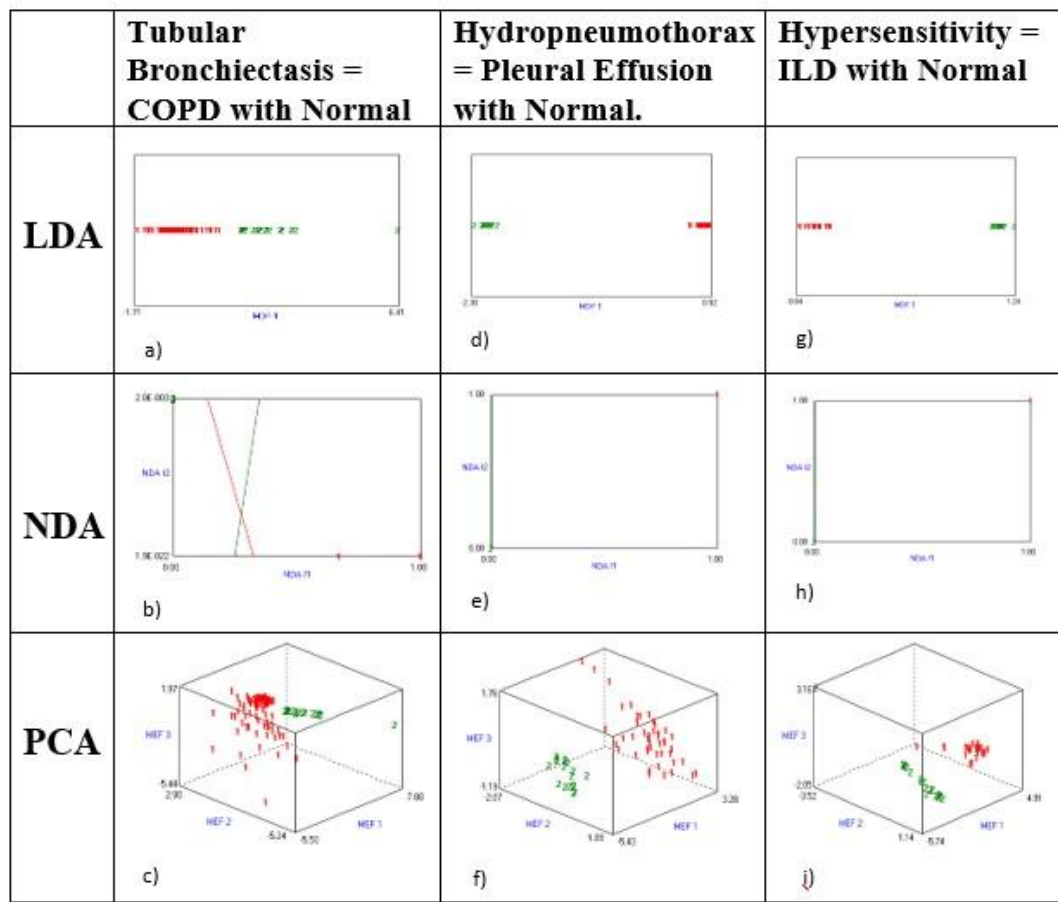


Figure 2 PCA, LDA, and NDA showing clear separation between normal and diseased lung tissues

Tubular Bronchiectasis is often a secondary structural manifestation of COPD. Chronic airway inflammation and mucus retention in COPD cause permanent bronchiolar dilation and airway wall thickening, leading to bronchiectasis changes. Hence, the presence of tubular bronchiectasis commonly reflects chronic airway obstruction and remodeling associated with COPD, a relationship also highlighted in recent HRCT-radiomics studies [16]. In this combination, Tubular Bronchiectasis (COPD) was compared with normal lung tissue using texture features extracted from HRCT images in MaZda. Following feature extraction, the Probability of Classification Error + Average Correlation Coefficient (POE+ACC) method was applied to select the ten most discriminative texture features for optimal separation between diseased and normal tissues. These selected features were subsequently used as input for dimensionality reduction and classification using Linear Discriminant Analysis (LDA), Nonlinear Discriminant Analysis (NDA), and Principal Component Analysis (PCA) methods.

3. Results

The LDA achieved 0.00% misclassification error, showing perfect linear separation between the two classes as shown in Figure 2(a). The red cluster (Tubular Bronchiectasis/COPD) and green cluster (Normal) were completely separated along the MDF1 axis, confirming that the selected features were highly effective for

linear classification. Using a one-class Artificial Neural Network (ANN), the NDA achieved 0% misclassification error. This demonstrates that NDA could capture subtle nonlinear texture variations, providing stronger class discrimination than LDA, consistent with recent machine-learning evaluations of COPD and bronchiectasis radiomics [17], as shown in Figure 2(b). PCA transformed all ten input features into six principal components and achieved 0% misclassification error. This indicates that although PCA retained the majority of data variance, it offered weaker class distinction since it is unsupervised, as shown in Figure 2(c). Overall, all three methods achieved perfect classification accuracy, with LDA and NDA showing superior discriminatory ability, confirming the reliability of POE+ACC-selected features.

Hydropneumothorax and Pleural Effusion were analyzed together because both involve pleural space abnormalities characterized by fluid and/or air accumulation. On HRCT, these conditions show similar pleural-based density changes and fluid-air interfaces, producing comparable texture patterns that justify their combined analysis. For this combination, I compared Hydropneumothorax and Pleural Effusion against Normal lung tissue. The POE+ACC method was again used to select the ten most effective features with the highest discriminatory capability between diseased and normal regions. These selected features were processed using LDA, NDA, and PCA for comparative analysis.

The LDA achieved 0.00% misclassification error, indicating strong linear separability between the pleural diseases and the normal lung. The clusters were distinct with minimal overlap, confirming the discriminative power of the selected features as shown in Figure 2(e). The one-class ANN used in NDA produced 0% misclassification error. The nonlinear network effectively captured the differences in texture distribution caused by fluid and air accumulation in pleural regions, providing perfect classification, in line with recent pleural-space radiomics literature [18], as shown in Figure 2(f). PCA achieved 0% misclassification error. Although the PCA plot showed some degree of overlap due to its unsupervised nature, it still successfully separated diseased and normal cases, reflecting consistent textural differences as shown in Figure 2(g). All three methods, LDA, NDA, and PCA, achieved 100% classification accuracy, but NDA and LDA demonstrated more effective discrimination between pleural diseases and normal lung tissue. The combination of POE+ACC-selected features and the ANN-based NDA model confirmed that texture analysis can accurately characterize pleural abnormalities.

Hypersensitivity Pneumonitis and Interstitial Lung Disease were analyzed together because both represent interstitial lung involvement characterized by fibrosis, ground-glass opacities, and diffuse parenchymal changes. Their overlapping pathological and radiological features on HRCT produce similar texture patterns, supporting their combined evaluation. In this combination, I analyzed Hypersensitivity Pneumonitis (HP) and Interstitial Lung Disease (ILD) against Normal lung tissue. Texture features were extracted and refined using the POE+ACC method, which selected the ten features with the highest potential for class separation. These were then used for LDA, NDA, and PCA classification.

The LDA method achieved 0.00% misclassification error, showing that the two classes were completely linearly separable. The resulting LDA plot showed clear clustering, with red points (HP + ILD) entirely distinct from green points (Normal) as shown in Figure 2(h). The NDA classifier, built using a one-class ANN, achieved perfect classification (0% misclassification error). This indicates that NDA effectively captured the complex nonlinear texture differences present in interstitial lung abnormalities, similar to recent radiomics-based ILD and HP classification reports [19], providing maximum separation accuracy as shown in Figure 2(i). PCA produced 0% misclassification error. Although PCA successfully grouped diseased and normal regions separately, some feature overlap was noted due to its unsupervised nature. It still effectively represented the texture variance between both classes as shown in Figure 2(j). These results confirmed that all three classifiers provided 100% correct classification, with LDA and NDA showing the strongest separation. The success of POE+ACC feature selection and one-class ANN analysis validates the

robustness of the extracted texture parameters in differentiating interstitial lung disease from normal parenchyma.

4. Discussion

The present study demonstrates that quantitative radiomics texture analysis of HRCT lung images—performed using the MaZda platform—can accurately differentiate a wide spectrum of pulmonary and pleural diseases, including Tubular Bronchiectasis (COPD-related), Hydropneumothorax with Pleural Effusion, and Hypersensitivity Pneumonitis with Interstitial Lung Disease (ILD). Extraction of more than 300 texture features from carefully selected ROIs enabled comprehensive characterization of parenchymal and pleural heterogeneity. The use of the POE+ACC feature selection method significantly improved model efficiency by identifying the most discriminative and least redundant texture features, consistent with contemporary radiomics optimization and feature-stability studies in pulmonary imaging[20].

Across all disease groups, the classification results obtained using PCA, LDA, and NDA indicated exceptional separability between normal and pathological lung tissues. The perfect (0.00%) misclassification rate achieved by LDA highlights the strong linear separability of POE+ACC-selected texture features for patterns associated with COPD-related airway distortion, pleural air–fluid abnormalities, and interstitial parenchymal disease. This observation is in agreement with recent radiomics investigations demonstrating that LDA continues to perform exceptionally well in structured HRCT radiomic datasets for COPD phenotyping, pleural disease characterization, and ILD differentiation [21].

NDA, implemented using a one-class artificial neural network (ANN), further enhanced nonlinear discrimination. Its perfect classification performance suggests the presence of complex, non-linear texture alterations in both pleural and interstitial lung diseases—particularly in ILD and hypersensitivity pneumonitis—where fibrosis, heterogeneous ground-glass attenuation, and reticular distortion generate higher-order spatial dependencies. ANN-based classifiers have been repeatedly reported to outperform classical statistical and shallow machine-learning approaches in detecting subtle interstitial abnormalities and in differentiating ILD subtypes on HRCT and chest radiography datasets [22]. The strong performance of NDA in this study reinforces the suitability of ANN-driven models for capturing subtle heterogeneity-driven disease signatures that are not fully separable using linear transformations alone.

Although PCA is an unsupervised method, it also achieved 0% misclassification error, indicating that the disease classes possessed intrinsically distinct radiomic signatures. However, visual inspection of the PCA projections revealed comparatively weaker class separation than that observed with LDA and NDA. This finding is consistent with recent HRCT radiomics literature, which consistently reports that PCA is highly valuable for variance exploration and visualization but generally inferior to supervised discriminant methods for definitive disease classification—particularly in conditions with overlapping radiographic manifestations such as pleural disease and interstitial pathology[23].

Importantly, this work directly addresses a critical gap in existing pulmonary radiomics research. Previous studies have typically examined isolated disease entities or limited diagnostic groups and often lacked standardized pipelines for feature selection and classifier comparison. Moreover, few investigations have systematically compared linear and nonlinear discriminant strategies using MaZda-derived texture features across multiple pulmonary and pleural disorders. By integrating POE+ACC feature selection with PCA, LDA, and ANN-based NDA within a single, unified analytical framework, the present study demonstrates that both linear and nonlinear discriminative radiomic signatures can be robustly extracted from HRCT data across diverse lung and pleural pathologies.

Through this approach, the study advances methodological consistency in pulmonary HRCT radiomics and provides evidence that MaZda-based texture analysis, when coupled with optimized feature selection and advanced discriminant models, can serve as a reliable, objective, and non-invasive adjunct to conventional radiological interpretation.

5. Conclusion

This study demonstrates that MaZda-based quantitative radiomics texture analysis of HRCT lung images provides a reliable, objective, and non-invasive approach for differentiating a diverse range of pulmonary and pleural diseases, including COPD-related airway abnormalities, pleural air–fluid pathologies, and interstitial lung disease. The integration of POE+ACC feature selection with PCA, LDA, and ANN-based NDA achieved perfect classification performance, underscoring the robustness and discriminative power of the proposed radiomic pipeline. The strong performance of both linear and nonlinear classifiers highlights the presence of distinct and complementary texture signatures across disease entities. These findings support the role of optimized texture analysis as a valuable adjunct to conventional radiological assessment and suggest its potential for enhancing diagnostic precision and decision support in clinical pulmonary imaging.

6. Acknowledgement

The authors acknowledge Bahawal Victoria Hospital, Bahawalpur, Pakistan, for the support and cooperation provided during the conduct of this research.

7. Author Contributions

Mehrun Nisa, Muhammad Saeed Ahmad (Conceptualization, Methodology, Investigation, Data Curation, Formal Analysis, Software, Validation, Visualization, Writing – Review & Editing)

Aliza Nadeem, Ayesha Amjad, Sehar Zafar, Aneeba Kanwal, Warda Afifa, Nimra Ejaz (Investigation, Data Curation, Validation, Visualization, Writing – Original Draft)

Hafiz Muhammad Amir Jamil (Resources, Investigation, Clinical Data Interpretation)

Naima Amin (Correspondence, Funding Acquisition, Conceptualization, Writing – Review & Editing)

8. Conflict of Interest: None

9. Source of Funding: None

References

- [1] Aneesh AB, Sonali B, Arun B, et al. Recent Advances in the Treatment of Interstitial Lung Diseases. *Cureus* 2023, 15(10):e48016. <https://doi.org/10.7759/cureus.48016>
- [2] Alvar A, Erik M, Dawn LD, et al. Pathogenesis of chronic obstructive pulmonary disease: understanding the contributions of gene-environment interactions across the lifespan. *Lancet Respir Med* 2022, 10(5):512-524. [https://doi.org/10.1016/S2213-2600\(21\)00555-5](https://doi.org/10.1016/S2213-2600(21)00555-5).

[3] Jiao X, Qingyue Z, Shuangqing L, et al. Inflammation mechanism and research progress of COPD. *Front. Immunol.* 2024, 15: 1404615. <https://doi.org/10.3389/fimmu.2024.1404615>.

[4] Rachid C, Hindi M, Fikri O, Amro L, FIKRI O. Diagnostic approach to hypersensitivity pneumonitis: a report of two cases. *Cureus* 2023, 15(8). <https://doi.org/10.7759/cureus.43290>

[5] Wijsenbeek M, Suzuki A, Maher TM. Interstitial lung diseases. *The Lancet* 2022, 400(10354):769-86. [https://doi.org/10.1016/S0140-6736\(22\)01052-2](https://doi.org/10.1016/S0140-6736(22)01052-2).

[6] Barnes H, Corte TJ, Keir G, et al. Diagnosis and management of hypersensitivity pneumonitis in adults: A position statement from the Thoracic Society of Australia and New Zealand. *Respirology* 2024, 29(12):1023-46. <https://doi.org/10.1111/resp.14847>.

[7] Bediwy AS, Al-Biltagi M, Saeed NK, et al. Pleural effusion in critically ill patients and intensive care setting. *World Journal of Clinical Cases* 2023, 11(5):989. <https://doi.org/10.12998/wjcc.v11.i5.989>.

[8] Vaghela D, Jasani DA, Patel RV, et al. Role of HRCT in the Diagnosis of Interstitial Lung Diseases: A CrossSectional Study of Radiological Patterns and Demographic Correlates. *European Journal of Cardiovascular Medicine* 2025, 15(6). <https://doi.org/10.5083/ejcm/25-06-54>

[9] Huang YY, Lin YC, Tsai SH, et al. Automated Computer-Assisted Diagnosis of Pleural Effusion in Chest X-Rays via Deep Learning. *Diagnostics* 2025, 15(18):2322. <https://doi.org/10.3390/diagnostics15182322>

[10] Barioni ED, Lopes SL, Silvestre PR, et al. Texture analysis in volumetric imaging for dentomaxillofacial radiology: transforming diagnostic approaches and future directions *Journal of Imaging*. 2024, 10(11):263. <https://doi.org/10.3390/jimaging10110263>

[11] Zubair AR, Alo OA. Grey level co-occurrence matrix (GLCM) based second order statistics for image texture analysis. *International Journal of Science and Engineering Investigations* 2019, 8(93). 89319-11. <https://doi.org/10.48550/arXiv.2403.04038>

[12] Orlhac F, Frouin F, Nioche C, et al. Validation of a method to compensate multicenter effects affecting CT radiomics. *Radiology* 2019, 1(1):53-9. <https://doi.org/10.1148/radiol.2019182023>

[13] Jacob C, Gopakumar C, Nazarudeen F. Optimized radiomics-based machine learning approach for lung cancer subtype classification. *Biomedical Engineering: Applications, Basis and Communications* 2023, 35(05):2350023. <https://doi.org/10.4015/S1016237223500230>

[14] Papadimitroulas P, Brocki L, Chung NC, et al. Artificial intelligence: Deep learning in oncological radiomics and challenges of interpretability and data harmonization. *Physica Medica: European Journal of Medical Physics* 2021, 83:108-21. <https://doi.org/10.1016/j.ejmp.2021.03.009>

[15] Chen W, Zhu J, Ni J, et al. Imaging Phenotypes Assessment by Using Quantitative Parameters for CT-Defined Subtypes of Chronic Obstructive Pulmonary Disease. *International Journal of Chronic Obstructive Pulmonary Disease* 2025, 20:1279-86. <https://doi.org/10.2147/COPD.S50509>

[16] Yang Y, Wang S, Zeng N, et al. Lung Radiomics Features Selection for COPD Stage Classification Based on Auto-Metric Graph Neural Net-work. *Diagnostics* 2022, 12(10): 2274. <https://doi.org/10.3390/diagnostics12102274>

[17] Xing ZC, Guo HZ, Hou ZL, et al. The value of computed tomography-based radiomics for predicting malignant pleural effusions. *Frontiers in Oncology* 2024, 14:1419343. <https://doi.org/10.3389/fonc.2024.1419343>

[18] Wang Y, Shang Y, Yao J, et al. Deep learning in interstitial lung disease: classification and prognostic insights. *Radiology Science* 2024, 3(01):41-9. <https://doi.org/10.15212/RADSCI-2023-0011>

[19] Chen H, Li W, Zhu Y. Improved window adaptive gray level co-occurrence matrix for extraction and analysis of texture characteristics of pulmonary nodules. *Computer Methods and Programs in Biomedicine* 2021, 208:106263. <https://doi.org/10.1016/j.cmpb.2021.106263>

[20] Zhang Y, Wang Y. Machine learning applications for multi-source data of edible crops: A review of current trends and future prospects. *Food Chemistry: X* 2023, 19:100860. <https://doi.org/10.1016/j.fochx.2023.100860>

[21] Bermejo-Peláez D, Ash SY, Washko G, et al. Classification of interstitial lung abnormality patterns with an ensemble of deep convolutional neural networks. *Scientific reports* 2020, 10(1):338. <https://doi.org/10.1038/s41598-019-56989-5>

[22] Ishida T, Katsuragawa S, Ashizawa K, et al. Application of artificial neural networks for quantitative analysis of image data in chest radiographs for detection of interstitial lung disease. *Journal of digital imaging* 1998, 11(4):182. <https://doi.org/10.1007/BF00897188>

[23] Nisa M, Buzdar SA, Javid MA, et al. Machine vision-based Statistical texture analysis techniques for characterization of liver tissues using CT images. *JPMA* 2022, 72(9):1760-5. <https://doi.org/10.47391/10.47391/JPMA.4138>